

UC San Diego

Capstone Papers

Title

Influence of Atmospheric River Precipitation on Vegetation Growth and Fuel

Permalink

<https://escholarship.org/uc/item/7v26b9qj>

Author

Campbell, Ian

Publication Date

2024

Data Availability

The data associated with this publication are within the manuscript.

**Influence of Atmospheric River Precipitation on Vegetation Growth and Fuel
Loading in Southern California**

Ian Campbell, Kristen Guirguis, Sasha Gershunov, Christine Albano

Signed by:

Abstract

In the last decade, research on atmospheric rivers (ARs) has surged due to their potential to cause extreme flooding and alleviate drought stress in the Western United States. Concurrently, wildfires in Southern California have become increasingly costly and destructive. While the timing of the first fall AR is known to influence wildfire risk in Southern California, the impact of ARs on spring vegetation growth and subsequent fall wildfire risk remains poorly understood, especially at the fine scale of Southern California ecosystems.

To investigate this link, we analyzed forty years of AR-associated Integrated Vapor Transport (IVT) and winter precipitation data across ten Level IV Ecoregions in Southern California. We examined the correlations between these metrics and the Enhanced Vegetation Index (EVI) and the Evaporative Demand Drought Index (EDDI). Our analysis revealed that productivity during the growing season is linked to the previous winter's total AR-associated IVT, and even more strongly to winter precipitation totals. We found positive correlations between AR-associated IVT and precipitation with EVI in early peak fire season (defined as August through October), particularly in chaparral-dominated areas, while conifer forests and grassland ecosystems displayed weaker correlations.

We also found that the 90-day EDDI in early peak fire season was influenced by winter precipitation in some ecoregions, and that EDDI also had significant correlations with early peak fire season EVI.

Our findings suggest that wet winters may increase wildfire risk in fuel-limited ecosystems like grasslands due to higher biomass accumulation, whereas in chaparral-dominated areas, increased moisture may reduce wildfire risk via maintaining higher fuel moistures in the fire season. These results underscore the need for further research to clarify the importance of fuel abundance versus fuel dryness, especially in conifer forest and sage scrub ecoregions for accurate Southern California wildfire risk assessment.

Introduction: Atmospheric Rivers (ARs)

Atmospheric rivers (ARs) are long, narrow bands of concentrated water vapor that play a crucial role in transporting moisture poleward from the tropics (Zhu & Newell 1998). They account for up to half of California's precipitation (Gershunov et al. 2017), which arrives primarily during the winter season. From year to year, California experiences the most highly variable precipitation of any state, primarily due to the presence or absence of ARs (Dettinger et al. 2011). This variability leads to significant environmental impacts, including influencing productivity in the growing season (Albano et al. 2017).

ARs predominantly occur from October to April, with stronger and more frequent occurrences in Northern California compared with Southern California. Despite this, they still deliver a significant portion of Southern California's precipitation (Albano et al. 2017,

Gershunov et al. 2017). As these moisture-laden air masses are pushed upward by mountains, orographic lifting causes them to cool and precipitate, leading to variable precipitation totals across different altitudes (Albano et al. 2020).

ARs are classified on a scale from 1 (beneficial) to 5 (hazardous), considering both the duration and Integrated Vapor Transport (IVT) of the AR (Ralph et al. 2019). Weaker ARs are primarily beneficial because they enhance water supply and snowpack without associated risks, while stronger ARs can lead to hazards like flooding and landslides (Ralph et al. 2006; Ralph et al. 2019; Corringham et al. 2019). These “rivers in the sky” provide essential water during the winter for various Southern California plant communities (Dettinger et al. 2011), mainly on the west/southwest facing slopes of coastal topography. This variability in vegetation growth affects wildfire fuel availability during the dry season when devastating fires can spread rapidly during downslope wind events (e.g. Santa Ana winds) starting in early fall (Westerling et al. 2004, Moritz et al. 2010, Kolden and Abatzoglou 2018, Gershunov et al. 2021).

Fire Relevance

Southern California faces complex fire-management challenges due to expanding major population centers adjacent to burn-prone ecosystems. While Northern California has seen most of the state’s recent large wildfires, Southern California has experienced many of the most structurally destructive fires (Syphard et al. 2019). Notable events include the Southern California wildfires of 2003, in which from just October 20th to November 3rd, 740,000 acres of land were burned, causing more than \$2 billion in property damage (Keeley et al. 2004). They also include the Fall 2007 California firestorm, where 17 major

wildfires destroyed over 1,500 homes, and the December 2017 fires, causing over three billion dollars in damages and forcing nearly a quarter million people to evacuate (Shi et al. 2019). The region's extensive wildland-urban interface (WUI) areas exacerbates the number of ignitions (Syphard et al 2007).

The region's Mediterranean climate, characterized by hot, dry summers and mild, wet winters, contributes to its wildfire susceptibility (Dong et al. 2022). While wildfires can occur year-round, they are most common from June to December. The drying of vegetation begins to speed up in June due to high temperatures and lack of rain (Chiariello and Field, 2004). Fuel moistures typically reach their lowest in fall and early winter following the extended dry period, which is exacerbated by the occurrence of Santa Ana winds. These downslope winds are not only extremely effective at drying fuels but can also lead to the rapid spread of wildfires due to their high wind speeds (Keeley et al 2021). The risk of large fires is generally reduced after autumn precipitation onset (Cayan et al. 2022). In this study, we focus on fuel moisture during August-October when vegetation typically reaches peak dryness before the onset of the rainy season.

Fuel Loading

Fuel loading refers to the accumulation of biomass, including forbs, grasses, shrubs, and trees during the peak growing season, which we found occurs as early as March-April in lower elevation ecoregions in Southern California and as late as June-July at higher elevations. The relationship between winter precipitation, vegetation growth, and fuel loading is complex. Some ecosystems, like xeric grasslands, are fuel-limited, meaning they

generally lack sufficient biomass to host large wildfires (Steel et al. 2015). In such areas, wet winters can increase fire severity by adding fuel to the landscape (Albano et al. 2017).

Conversely climate-limited regimes are those in which sufficient fuel is usually present for fires to occur, but fuel moisture or atmospheric moistures are too high for combustion during normal conditions (Steel et al. 2015). These include ecosystems such as rainforests, where a dry winter can increase wildfire risk by reducing fuel moisture, while not limiting the availability of biomass. Southern California ecosystems exhibit features of both regimes, with California grasslands being the most fuel-limited, Southern California conifer forests somewhat fuel-limited, and chaparral more climate-limited (Steel et al, 2015). In general, it has been shown that fire activity has a higher likelihood of occurring in areas where biomass differential between spring and summer values is high, and that the annual fuel can be closely correlated with annual precipitation (Li et al. 2021).

Floral Biodiversity

Southern California hosts a rich variety of plant species, including many threatened endemic species such as the critically endangered Torrey Pine (*Pinus torreyana*), Catalina Ironwood (*Lyonothamnus floribundus*), and Santa Rosa Island Manzanita (*Arctostaphylos confertiflora*). Development has fragmented biomes, and changes in fire regimes over recent decades threaten sensitive forest and chaparral habitats. In some conifer plant communities, fire suppression has led to fuel accumulation, resulting in more intense and frequent fires (Goforth et al. 2008). Old growth chaparral, adapted to low fire frequencies,

faces threats from frequent accidental ignitions and controlled burns, which can lead to type-conversion to non-native weedlands (Guiterman et al. 2022).

Climate change may also enhance wildfire risk by creating favorable conditions for invasive species, increasing plant water stress, and promoting the spread of nonnative plants that alter fire regimes. Rising temperatures and drought conditions exacerbate these issues. Climate change may also affect AR behavior, potentially making them stronger, wider, and longer-lasting as global temperatures rise (Gershunov et al. 2019), though this trend has not yet been observed (Williams et al. 2024).

Level IV Ecoregions Background

The ten ecoregions were chosen due to their susceptibility to wildfires and their diverse plant communities with varying natural fire regimes (Figure 1). Many of these ecoregions are also located at the wildland-urban interface (WUI), making them critical areas for developing a better understanding of fire risk to protect lives and property. Even the selected ecoregions not directly at the WUI can still ignite fires that spread across ecoregions to major population centers or detrimentally affect the population through wildfire smoke exposure (Aguilera et a. 2023). This is because the fall Santa Ana winds blow from the east/northeast, and most of these ecoregions are situated east/northeast (e.g. upwind) of Metropolitan San Diego and Los Angeles. Historically, many of Southern California's most structurally damaging fires originated in wilderness areas. For instance, the Cedar Fire (October-November 2023), which ultimately destroyed hundreds of homes in the Scripps Ranch community of San Diego, started 30 miles to the east in the Cuyamaca Mountains (ecoregion 8f, Figure 1).

Selected Level IV Ecoregions Map and Key

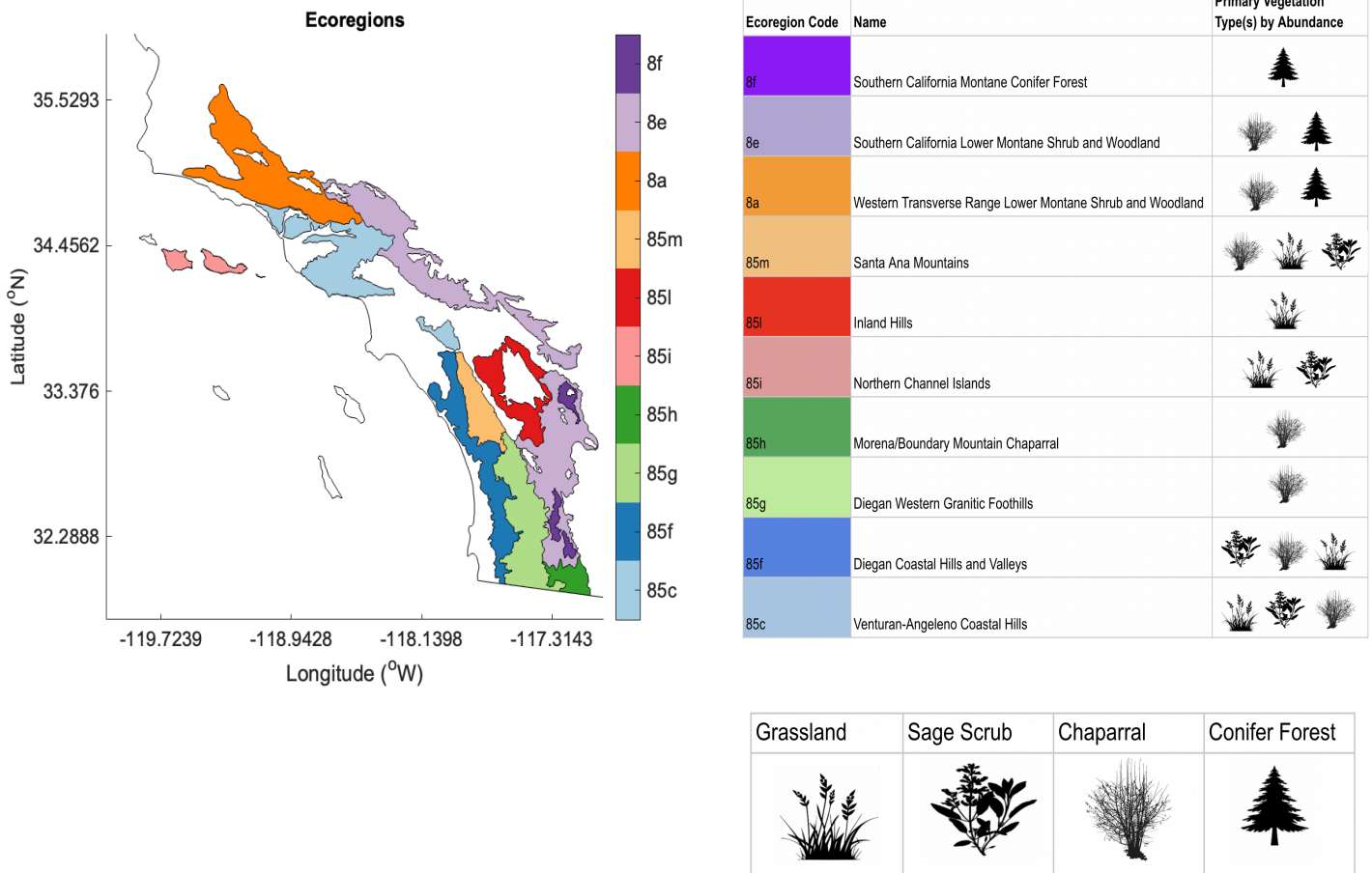


Figure 1a: The ten selected ecoregions and their predominant vegetation types

These ecoregions span from San Diego County’s border with Mexico, north to Santa Barbara County (Figure 1a). We have sorted them into their primary vegetation types, in order of relative abundance. Despite their ecological significance, Oak Woodlands were not

considered due to their relatively small extent within the ecoregions. Additionally, despite the existing diversity of chaparral types, from chamise chaparral to montane chaparral, chaparral was consolidated as a single category for simplicity. The same is true for grasslands, which can encompass both annual and perennial grasslands, but for the purpose of this study were consolidated. Photographs highlighting vegetation in different ecoregions are shown in Figure 1b.



Figure 1b. Photographs of vegetation in selected ecoregions. (A) The sparsely vegetated eastern edge of the Morena/Mountain Boundary Chaparral. (Source: Hipcamp). (B) The relatively lush Santa Monica Mountains, of the Venturan-Angelino Coastal Hills ecoregion. (Source: Western National Parks Association). (C) The Northern Channel Islands is home to coastal sage scrub, which “dries out” by mid-summer. (Source: National Park Service). (D) Mount Laguna, in The Southern California Montane Conifer Forest, retains most of its greenness through the fall (Source: Cool San Diego Sights).

Selected Level IV Ecoregions Flora

The following descriptions provide greater detail on the vegetation found across the ten selected Level IV Ecoregions (Griffith et al. 2016).

85c- Venturan-Angelino Coastal Hills- Annual grassland, California sagebrush, California buckwheat, mixed sage, chamise chaparral, mixed chaparral, and coast live oak.

85e- Diegan Coastal Terraces- Coastal sage scrub, with maritime succulent, Diegan coastal sage scrub, and chaparral communities. California sagebrush, California buckwheat, black sage, ceanothus, coast live oak, and annual grasslands occur. A few vernal pools remain, as well as a small coastal stand of rare Torrey pines.

85f- Diegan Coastal Hills and Valleys- Vegetation includes coastal scrub and chaparral, annual and perennial grasslands, and some small pockets of coastal oak woodlands.

85g- Diegan Western Granitic Foothills- Typical vegetation includes foothill needlegrass, coast live oak, chamise, mixed chaparral, and California sagebrush.

85h- Morena/Boundary Mountain Chaparral- Vegetation is predominantly mixed chaparral and some chamise.

85i- Northern Channel Islands- Annual grassland, coastal sage scrub, and chaparral are typical, with some scattered mixed broadleaf woodland, island oak and coastal live oak woodlands, and a few Bishop or Torrey pine stands on sheltered slopes and canyons, or on ridges exposed to frequent fogs.

85m- Santa Ana Mountains- Mixed and chamise chaparral, coastal sage scrub, coast live oak, and areas of annual grassland. Some canyon live oak occurs, bigcone Douglas-fir is found at the heads of some canyons, and sparse stands of Coulter pine are at high elevations. In the southeast, the Santa Rosa Plateau supports areas of vernal pools, native grasslands, and some Engelmann oak woodlands.

8a- Western Transverse Range Lower Montane Shrub and Woodland- The climate has more marine influence than Southern California Mountain regions farther inland. Elevations range from about 1,000 to more than 6,000 feet. Some coastal sage scrub occurs at low elevations. Scattered patches of coast live oak, canyon oak, Coulter pine, California bay, or bigcone Douglas-fir occur in a mostly chaparral-dominated landscape of chamise, ceanothus, manzanita, and scrub oaks, with smaller populations of other species such as cherry and birchleaf mountain-mahogany.

8e- The Southern California Lower Montane Shrub and Woodland ecoregion- Chaparral-dominated landscape also containing patches of mixed evergreen woodland consisting mostly of bigcone Douglas-fir and canyon live oak. These fragmented, compact groves typically occur in deep canyons and on steep north-facing slopes. Some minor areas

of coastal sage scrub occur near the lower margins. The mosaic of land cover and vegetation communities is complex. Certain chaparral shrubs in the Peninsular Ranges, such as mission manzanita and red shank, have limited ranges in southern California and Baja California. Other shrubs, such as California buckwheat, are ubiquitous.

8f- Southern California Montane Conifer Forest- Mixed coniferous forest with ponderosa pine, Jeffrey pine, sugar pine, white fir, incense cedar, hardwoods such as canyon live oak and black oak, and areas of montane chaparral. Ponderosa pine tends to be limited to moist areas with deeper soils, with extensive stands occurring in the western San Bernardino Mountains and on the western slope of San Jacinto Mountain.

Data Collection

- Level IV ecoregions were defined using the California Level IV Ecoregion shapefile from the US EPA database.
- AR associated IVT data from October 1983 to April 2023 was collected from an AR catalog (Gershunov et al 2017)

The following data was downloaded from ClimateEngine.org

- Temperature data were taken using NCLIM monthly data, and the annual mean was calculated for each ecoregion (Vose et al. 2024).
- Precipitation data were taken from Climate Hazards Group InfraRed Precipitation (CHIRPS) Pentad 4.8km from October 1983 to April 2023 (Funk et al. 2015).

- Enhanced Vegetation Index (EVI) measurements were taken from Landsat 5/7/8/9 measurements from January 1984 to December 2023. EVI measurements are sporadic but generally available biweekly to pentad (courtesy of the U.S. Geological Survey)
- 30 and 180 day Evaporative Demand Drought Index (EDDI) data were taken from the GridMET Drought 4km Pentad database from January 1984 to December 2023 (Abatzoglou 2011).

Methodology

We use records of precipitation during AR-season (October - April) from 1983 to 2023, defined as winter precipitation (WP), along with cumulative AR associated IVT, to quantify the relative wetness of a winter.

We use EVI to quantify vegetation greenness throughout the year, focusing on the growing season and the early peak fire season (August-October). Many previous studies have used the Normalized Difference Vegetation Index (NDVI) to measure vegetation greenness, but EVI is better suited to dense vegetation, and corrects for atmospheric conditions (Huete et al. 2002). In this study, we take the mean of the five highest EVI values from each March-July to quantify vegetation growth. Additionally, we take into account the possibility for erroneous measurements by removing all EVI values above 0.5 or below 0 before analysis. An EVI below zero would indicate no detectable vegetation or the abundance of snow. All ecoregions were vegetated, and snow should not have been abundant during the peak growing season at any of the ecoregions. An EVI above 0.5 would

be more than three standard deviations away from the mean in all ecoregions, and would be more expected in lush forests or agricultural regions (Huete et al 2006).

While other studies have used a single peak NDVI value to quantify vegetation growth, we found that taking a larger sample size helps to reduce the high-frequency noise arising from daily variability and does a better job of capturing the seasonal growing season more comprehensively. Additionally, this approach minimizes the possibility of data error, and accounts for the fact that different plant types within the same ecoregion can reach peak greenness at different times of the year. By not defining a growing season, rather taking the five highest values from March-July, we allow for flexibility for the growing season to occur at different times of the year, both between ecoregions and from year to year. For instance, lower elevation ecoregions may experience peak productivity in March one year and April the next year, while higher elevation ecoregions may experience peak productivity in June one year and then July the next year.

To measure greenness during the fire season, the average EVI from August-October was quantified. Though early winter months (November and December) are also high wildfire risk months in Southern California, they were not considered because the relationship between EVI in these months and the previous rainy season (the focus of this study) is complicated by the onset of the next AR season..

To understand how the influence of summer atmospheric conditions on fire season EVI compared to the influence of the previous winter's precipitation, we also considered EDDI. EDDI is calculated using four variables- temperature, wind, humidity, and solar radiation, and estimates the anomalous evaporative demand, or "thirst", from the atmosphere (Hobbins et al. 2016). The 180-day and 90-day EDDI data represent

anomalous evaporative demand from the last six months and three months respectively. These EDDI measurements from August to October of each year were isolated, and their mean was taken. Thus, the 180-day EDDI represents the anomalous evaporative demand from February to October, while the 90-day EDDI considers June to October.

To understand the link between WP, IVT, EDDI, and EVI, Spearman Rank Correlations Coefficients were calculated.

Results

Climatology

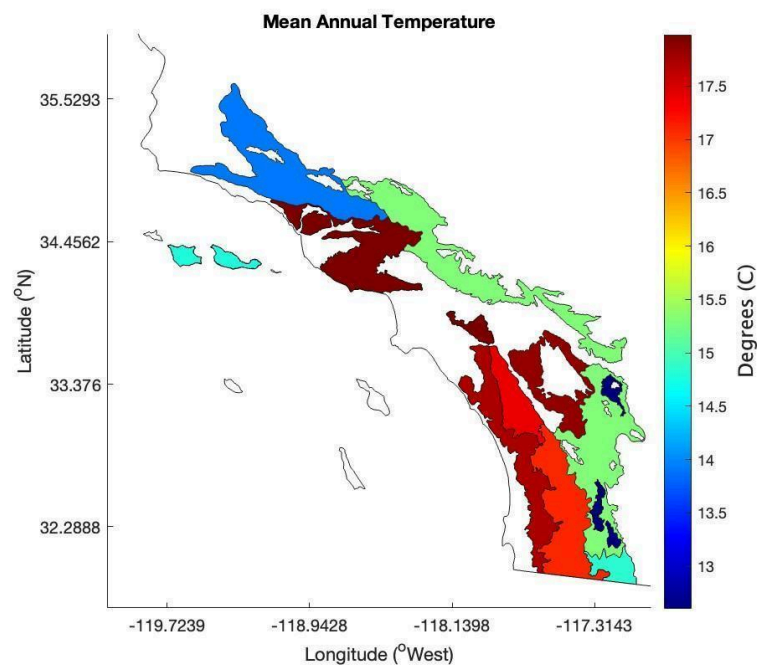


Figure 2: Mean Annual Temperature

Despite their relatively close geographic distribution, these ten ecoregions experience distinct climates. The calculated mean annual temperature from 1984-2023

amongst the ecoregions ranged from just 12.6 C in the Southern California Montane Conifer Forest to 18.0 C in the Venturan-Angelino Coastal Hills. Though there is variability within each ecoregion, this map shows their average.

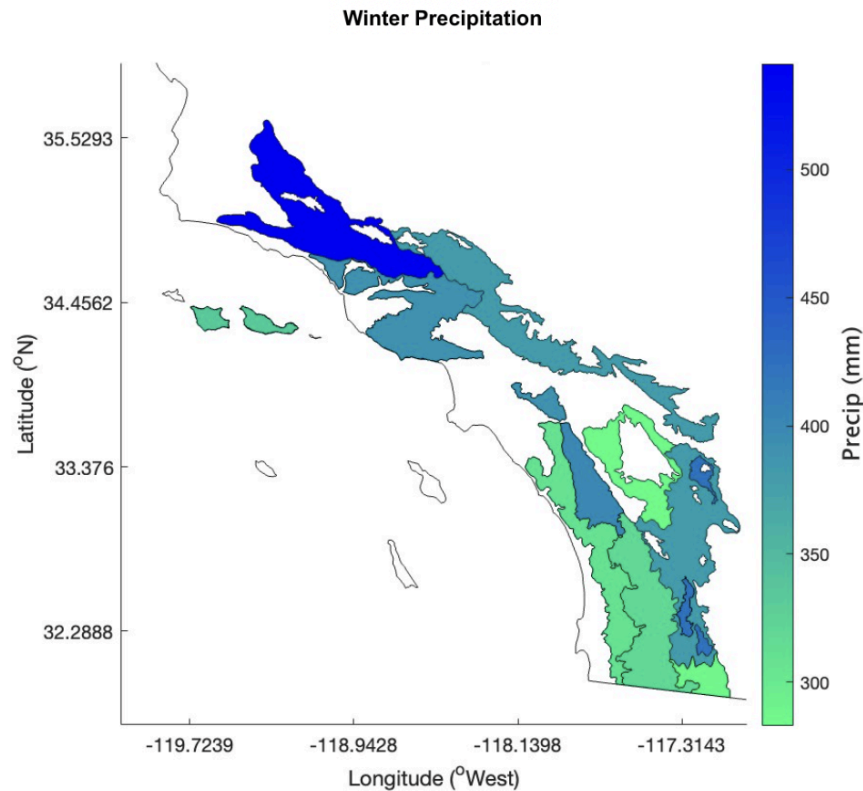


Figure 3: Mean Winter Precipitation

The mean winter precipitation (WP) ranged from 283 mm in the Inland Hills to 541 mm in the Western Transverse Range Lower Montane Shrub and Woodland. Overall, there is a negative correlation between mean temperature and precipitation of -0.48 when considering all of the ecoregions, meaning the warmer ecoregions also tend to experience less winter precipitation than the cooler mountainous ecoregions. This can partially be attributed to the orographic lifting of ARs leading to higher precipitation in cooler

mountainous areas. Adding to this relationship is the fact that ecoregions to the north, which are typically cooler, experience more precipitation from ARs (Gershunov et al. 2017). This can be partially attributed to their closer proximity to the typical prevailing westerly jet stream which steers ARs, as well as the greater prevalence of frontal cycles which are associated with 82% of ARs (Zhang et al. 2019).

Plant Productivity

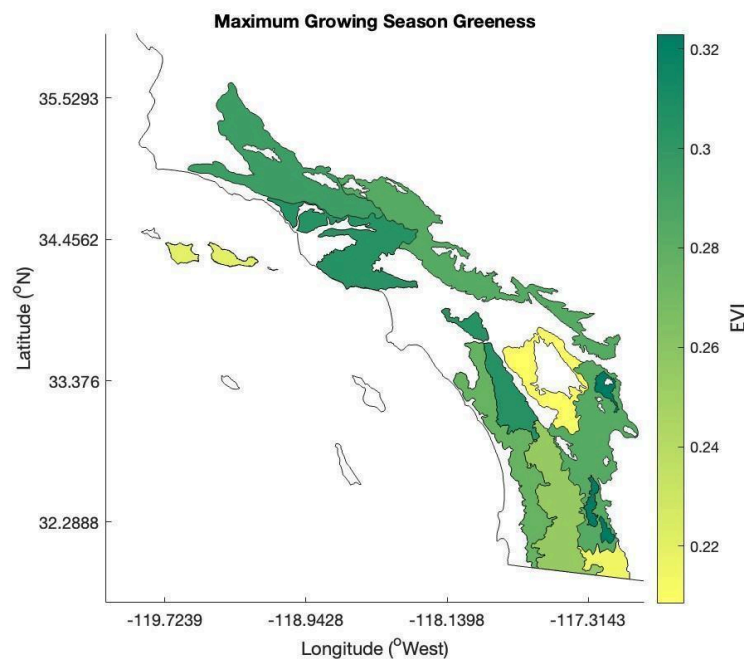


Figure 4: Maximum Growing Season Greenness

The mean of the five maximum March-July EVI values also varied greatly across ecosystems from 0.21 in the Inland Hills to 0.36 in the Southern California Montane Conifer Forest (EVI scale range from brown (-1) to green (1)). These values represent the relative greenness and vegetation density at the peak of the growing season. Higher EVI values are

associated with greater productivity. The Inland Hills is a relatively hot and dry ecoregion, dominated by grasses. The low EVI value signifies relatively low biomass, as expected in a grassland. Conversely, the high EVI value in the conifer forests represents the relative abundance of biomass. We also see high EVI growing season values in the Santa Ana Mountains and the Venturan-Angeleno Coastal Hills. Both of these ecoregions are incredibly biodiverse and host three of the four main vegetation types (grassland, chaparral, and sage scrub). Additionally, both have small pockets of conifer forest. All of these vegetation types may experience peak productivity at different times within the same ecoregion. Because the methodology for quantifying growing season productivity uses a sample of the five highest EVI values, the mixed vegetation within some ecoregions results in an extended period of peak productivity. Therefore, these highly diverse ecoregions yield large EVI values when averaged over March-July because the productivity of each vegetation type is adding to the overall productivity. For instance, an ecoregion may display high productivity if it contains grasses which may reach peak productivity in March, and Chaparral and Sage Scrub which may reach peak productivity in April.

Chaparral dominated ecoregions, such as the Diegan Western Granitic Foothills (ecoregion 85g, Figure 1), experience moderate vegetation productivity during their growing seasons, which generally peaks from April to mid-May. Mixed vegetation regions that are Chaparral dominated (e.g., ecoregions 8e, 8a, 85m) experience moderate to high productivity. The exception for chaparral ecoregions is the Morena/Boundary Mountain Chaparral (85h), which generally displays low growing season productivity. This is because the chaparral community in this ecoregion is less dense, and the ecoregion experiences relatively low precipitation (Figure 3).

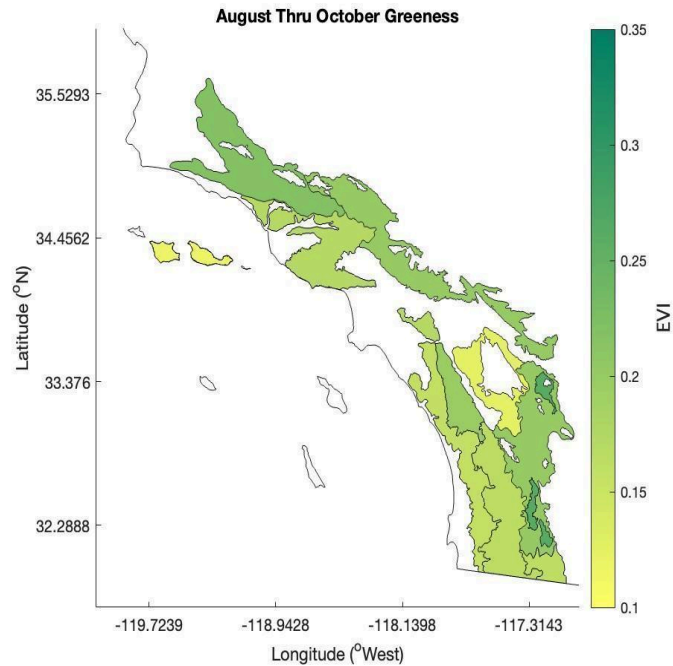


Figure 5: August Through October Average Greenness

The mean EVI from August-October, represents the greenness/density of vegetation at the beginning of fire season (Figure 5). The average EVI values for the Northern Channel Islands (85i) and the Inland Hills (85l) are both extremely low, at 0.11 and 0.12 respectively. These values reflect the abundance of grasses in these ecoregions, which adapt to the dry Mediterranean summers by reducing their metabolic activity, leading them to turn from green to brown (dos Santos et al. 2022). By contrast, the Southern California Montane Conifer Forest (85f) remains the greenest ecoregion at 0.26. Compared to grasses, conifer forests have deep and extensive root systems that can access water stored deep in

the soil, allowing them to sustain themselves during dry periods (Barbeta et al. 2014). Additionally, conifers store water in their sapwood and other tissues, which they can use during times of drought, helping them stay green (Waring and Running, 1978). Finally, the needles of conifers have a waxy coating that reduces water loss through transpiration (Provost et al 2013). Most chaparral ecoregions also maintained greenness relatively similar to their growing season peak. California chaparral is constituted largely of woody shrubs and herbaceous annuals, which unlike perennials develop complex root systems which allow them to retain much of their greenness year round (Rundel 2018).

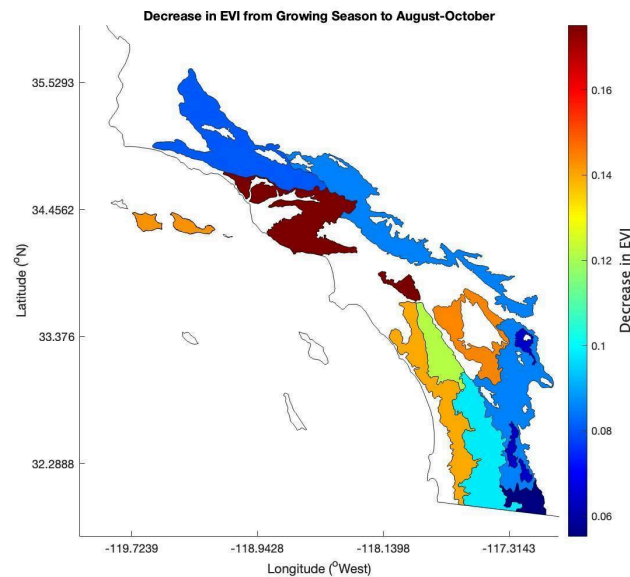


Figure 6: Change in EVI from Growing Season to August-October

It has been shown that fire activity can have a higher likelihood of occurring in areas where the NDVI differential between spring and summer values was especially high (Li et al. 2020). Therefore, we investigate this spring-to-fall differential in different ecoregions to

gain a better understanding of this contribution to wildfire hazard in Southern California. The mean difference between the peak EVI during March-July and the EVI during August-October represents the drying of vegetation from the growing season to fire season. It has been shown that fire activity can have a higher likelihood of occurring in areas where the NDVI differential between spring and summer values was especially high (Li et al. 2020). For the purpose of this study, we assume the same concept generally applies for EVI thanks to its similarity with NDVI.

As expected, all ecoregions experience statistically significant “browning” from the growing season to the fire season as indicated by the overall decrease in EVI (Figure 5). However, there is variation across the ecoregions in the quantity of this browning. In the Morena/Boundary Mountain Chaparral (85h), there was a relatively small average change of 0.05. By contrast, the Venturan-Angeleno Coastal Hills (85c), which is a grassland and sage scrub dominated ecoregion, exhibited a much larger mean difference in EVI of 0.18. This relationship is also seen for other grassland and sage scrub dominated hot ecoregions such as the Inland Hills (85l) and the Northern Channel Islands (85i), which also saw large average changes in EVI from their growing season to fire season.

The smallest changes tend to occur in the cooler ecoregions with greater portions of forest such as the Southern California Montane Conifer Forest ecoregion (8f). In part, this may represent the later growing seasons in these mountainous ecoregions, leaving less time to dry out before August-October. Additionally, it likely reflects the adaptation of conifer forests to maintain their green needles throughout the year, whereas grasslands and sage scrub typically “dry out” by mid-summer. In chaparral dominated ecoregions, the change in EVI was on average low to moderate, signifying less average annual drying than

ecoregions with an abundance of grasses and sage scrub, but more drying than in the heavily forested ecoregions.

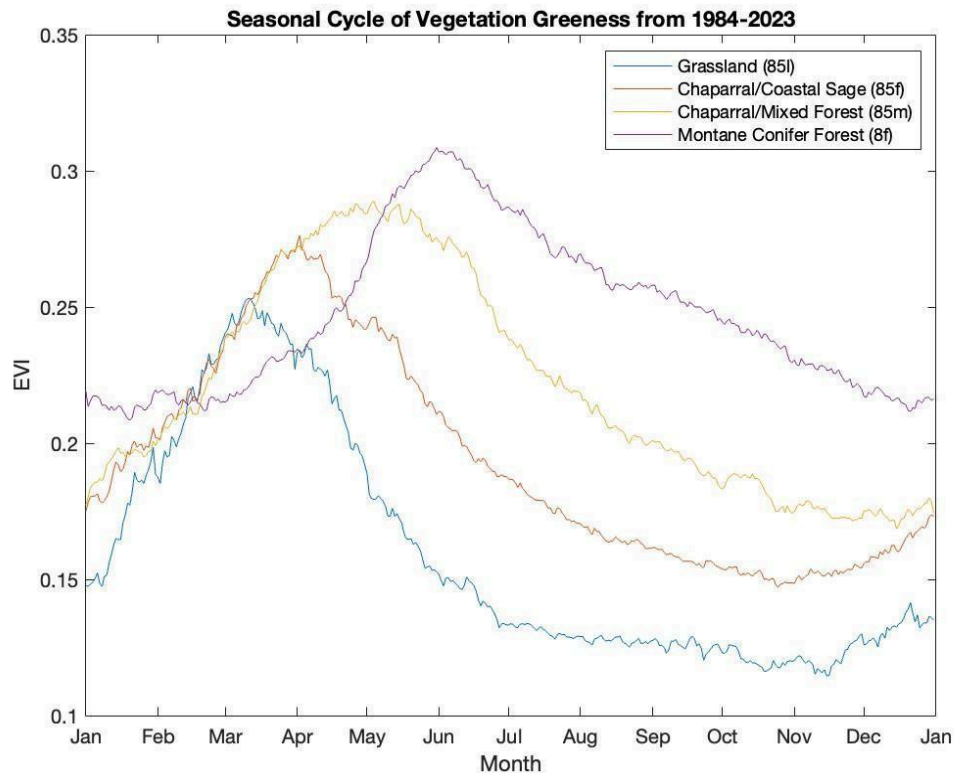


Figure 7: Average seasonal cycles of vegetation greenness across four ecoregions

The selected mean seasonal cycles represent the average EVI from the years 1984 to 2023 across four selected ecoregions. The four ecoregions range from relatively dry and hot to relatively wet and cool in the following order: the Inland Hills (85i), the Diegan Coastal Hills and Valleys (85f), the Santa Ana Mountains (85m), to the Southern California Montane Conifer Forest (8f). Their vegetation types range from primarily grassland, to coastal sage/chaparral, to chaparral/mixed forest, to montane conifer forest. There is a clear

pattern of cooler and wetter ecoregions exhibiting greater overall and peak EVI across the 40 years, and experiencing later growing seasons on average. This graph also illustrates why we see less change between growing season EVI and August-October EVI in cooler ecoregions, as there is less time after the growing season for the vegetation to dry out.

Key Findings

Winter Precipitation and EVI

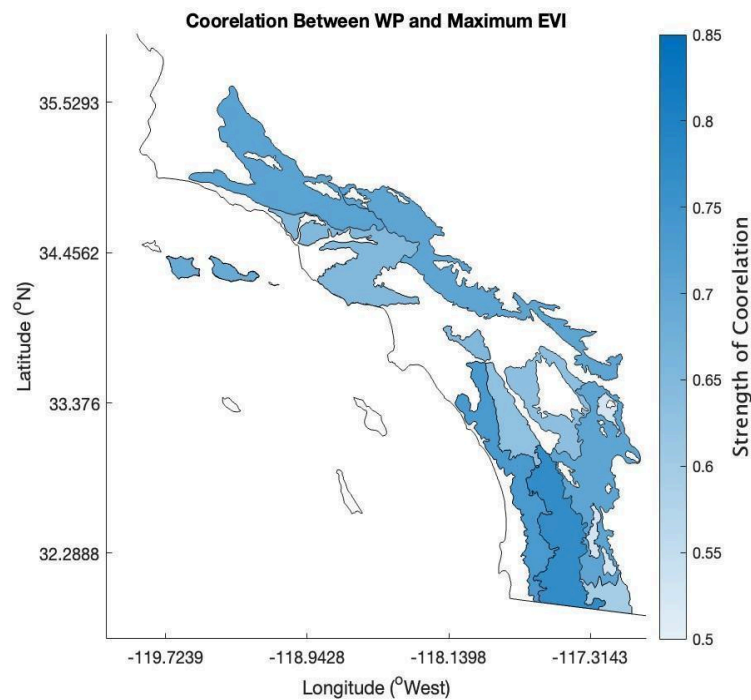


Figure 8: Correlations between winter precipitation and annual maximum 5 EVI values

The strength of the correlation between WP and the “interannual” growing season productivity ranged from a low of 0.52 in the Southern California Montane Conifer Forest to a high of 0.77 in the Diegan Western Granitic Foothills. There are generally frequent enough

EVI measurements that the highest values during March-July correspond to the true growing season (for instance, March-April in the hot Inland Hills). In general, the growing season EVI in ecoregions at moderate altitudes with greater chaparral dominance exhibited a strong correlation to the previous winter's precipitation. By contrast, both the driest/lowest (primarily sage scrub and grassland) and the highest/coolest (primarily conifer forest) ecoregions displayed relatively weak, but still statistically significant (at 1%), correlations between WP and growing season EVI.

This may indicate that chaparral is highly sensitive to anomalously dry winters, and grows relatively little, while after wet winters chaparral responds with high growth rates. For grasslands, sage scrub, and forest, these results may be interpreted as an indication that anomalously wet and dry years have less of an impact on growing season productivity. These results are surprising for the lower and drier grassland and sage scrub ecosystems, where one may expect a higher correlation between precipitation and growing season productivity. The lower correlation may be explained by the relatively short growing seasons in these ecoregions, which may be captured by one or two EVI measurements, but when the average of the top five EVI measurements is taken, the relationship is less apparent.

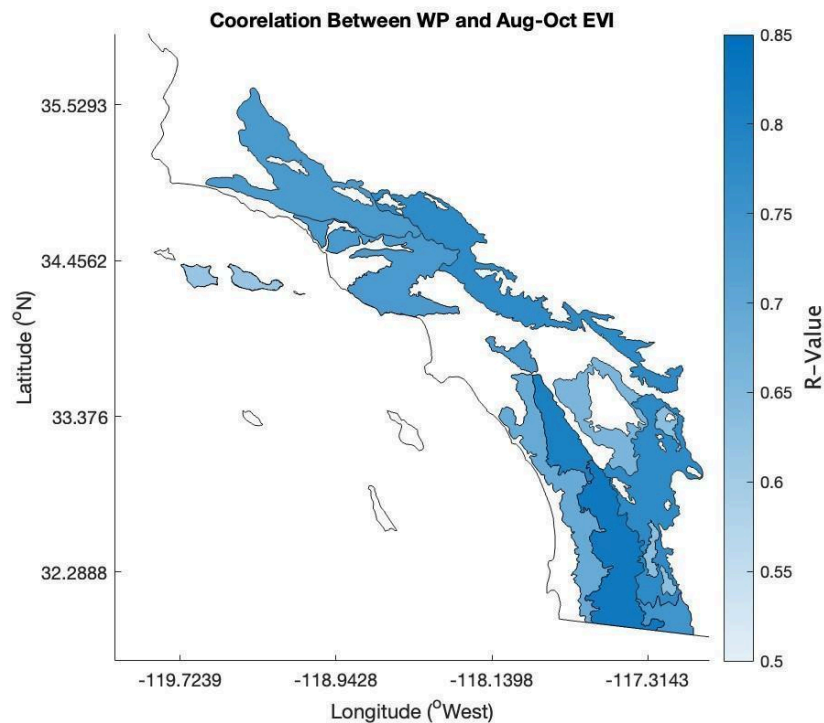


Figure 9: Correlations between winter precipitation and August through October EVI

The correlation between annual WP and mean August-October EVI values ranged from 0.61 in the Northern Channel Islands to 0.82 in the Diegan Western Granitic Foothills. In most ecoregions, the correlation between August-October EVI and WP was stronger than the correlation with the growing season EVI and WP. This suggests that the greenness of plant communities becomes more sensitive to the previous winter's precipitation several months after the end of the rainy season. The results suggest that chaparral dominated ecosystems remain the most sensitive to the quantity of the previous winter's precipitation going into the fire-season. After wet winters, chaparral is especially green during the fire season, while after dry winters it is especially brown.

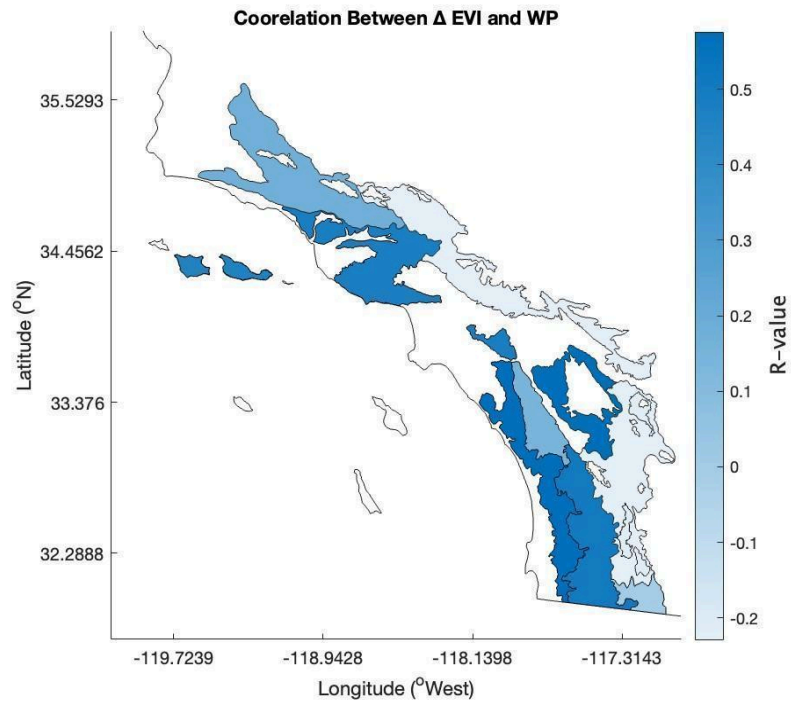


Figure 10: Correlation between the change in EVI (Aug-Oct minus Mar-July) and the previous winter's precipitation

The correlation between mean WYP and Δ EVI from the growing season to August-October ranged from insignificant in the more mountainous ecoregions to significant in the lower elevation, more grassland dominated ecoregions. Again, the growing season EVI was measured as the mean of the five highest EVI values that occurred from March to July, so the timing of these values is flexible and later in the mountainous ecoregions. Therefore, the lower correlations in the higher elevation ecoregions (figure 10) may be influenced by the shorter drying period between the growing season and August-October.

These results signify that in wetter years in grassland dominated ecoregions, there is greater relative fuel availability for more severe wildfires. This reflects earlier findings that wetter winters often lead to greater wildfire risk in more arid regions such as the great basin (Albano et al. 2017), where ecosystems are generally more fuel limited. By contrast, in the mountainous ecoregions, more climate limited ecoregions, there is no obvious parallel between fuel loading and precipitation in the same year. This result reflects earlier findings that there is no correlation between winter precipitation and wildfire risk in montane Southern California (Albano et al. 2017).

EVI and EDDI

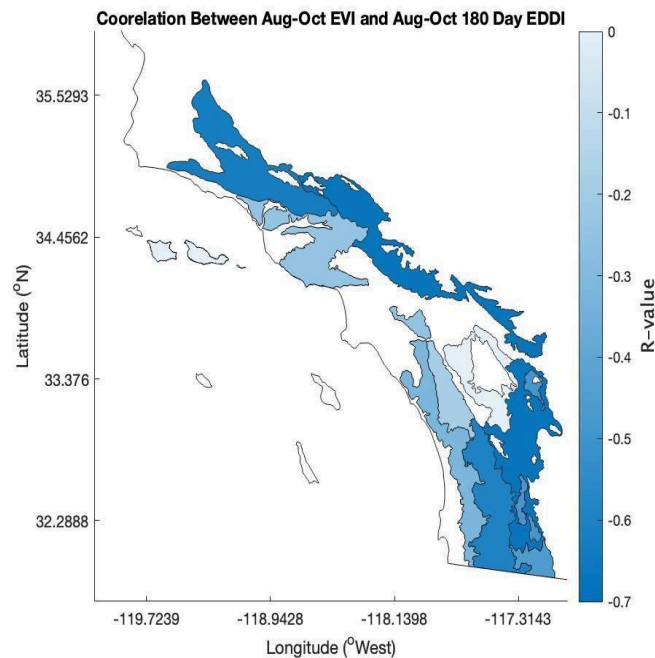


Figure 11: Correlations between August through October EVI and 180-day EDDI

The correlation between mean August-October EVI values and mean August-October 180-day EDDI and 90-day EDDI values represents the relationship between the atmospheric conditions aggregated over the prior six months and three months respectively, and the fire-season vegetation greenness measured across an ecoregion.

When considering the correlations between 180-day EDDI and fire season EVI, this relationship between is the strongest in the Southern California Lower Montane Shrub and Woodland (8e), with an R-value of -0.66, and was also relatively strong in the Diegan Western Granitic Foothills (85g), with an R-value of -0.59. This indicates plant health in these ecosystems are sensitive to spring and summer evaporative demand.

The relationship was insignificant in the more grassland-dominated ecoregions of the Northern Channel Islands (85i) and the Inland Hills (85l), signifying that by August, grasslands return to a similar level of brownness regardless of spring and summer evaporative demand.

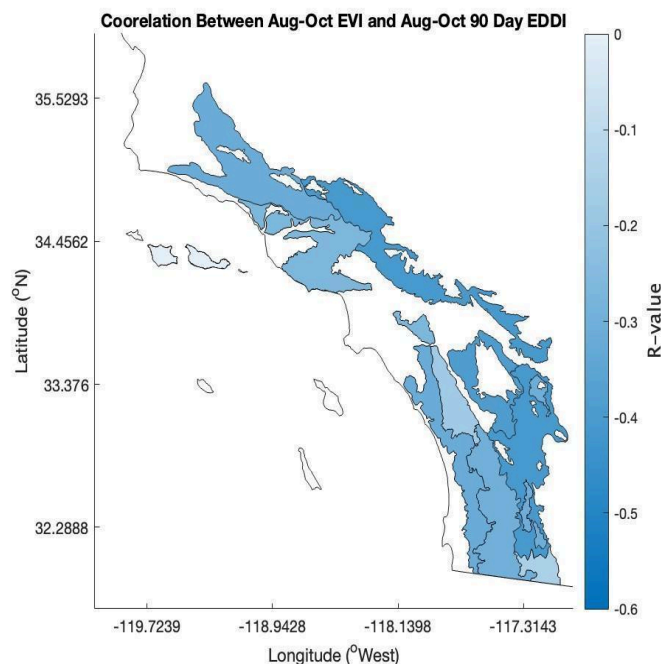


Figure 12: Correlations between August through October EVI and 90-day EDDI

Similar patterns were observed when using the 90-day EDDI metric, though with overall weaker relationships between August-October EVI and the 90-day EDDI. This indicates that the greenness of most vegetation communities in Southern California is impacted by the spring evaporative demand in addition to summer evaporative demand. Interestingly, in the Inland Hills (851), one of the ecoregions where there was no significant relationship between EVI and 180-day EDDI, there was a significant relationship when using the 90-day EDDI. This suggests that this hot grassland ecoregion is more impacted by short term evaporative demand conditions than long term drought conditions. This may reflect the inability of grasslands to store water for longer periods of time.

Winter Precipitation and EDDI

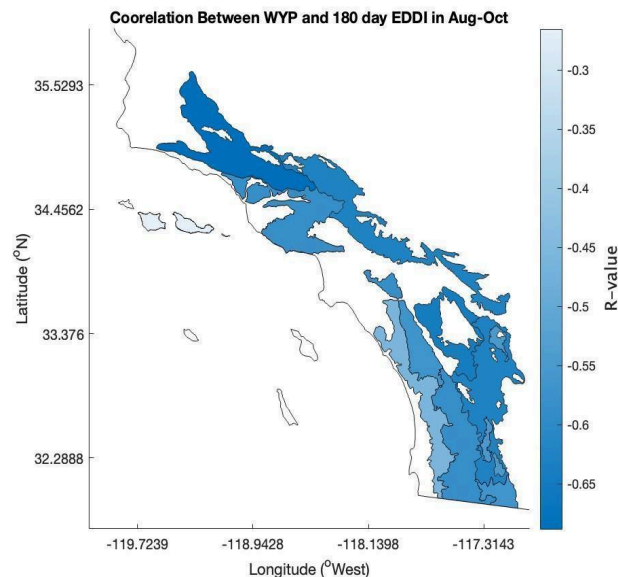


Figure 13: Correlations between Winter Precipitation and August-October 180 day EDDI

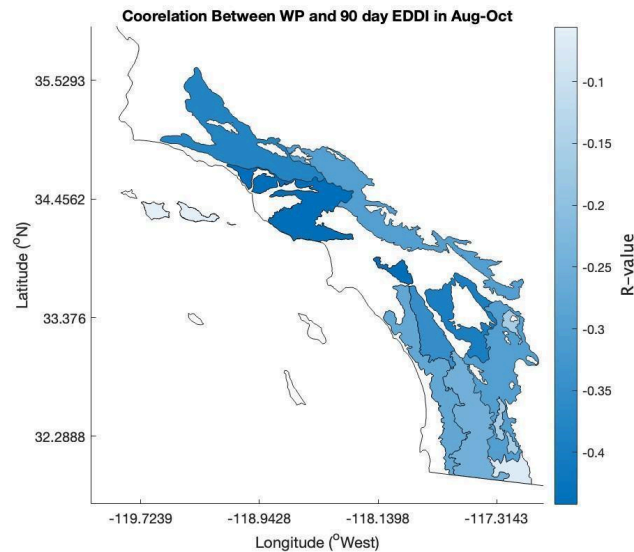


Figure 14: Correlations between Winter Precipitation and August-October 90 day EDDI

The relationship between winter precipitation and the EDDI is complex due to the complementary nature of their relationship (Bouchet 1963). The more significant the correlation between the two, the more significant the complementary relationship (CR) between vegetation communities and the atmospheric boundary layer (the part of the atmosphere that is directly impacted by conditions on the earth's surface). It is established that the CR is usually most apparent in water limited regions, where drought increases air temperature and lowers humidity levels due to the lack of precipitation and subsequent lack of evapotranspiration. This further lowers humidity at the boundary layer, enhancing drought conditions (Hobbins et al. 2016). Conversely, if vegetation communities have adequate available moisture to evapotranspire, evaporative demand remains relatively low because higher humidity is maintained by the evapotranspiration process. The low correlation between WP and EDDI observed in the Northern Channel Islands could be due

to the influence of fog and coastal low clouds, which can play a significant role in delivering moisture to Coastal California vegetation particularly in the summer months (Rastogi et al. 2016, Clemesha et al. 2021).

Application to Recent Observed Wildfires

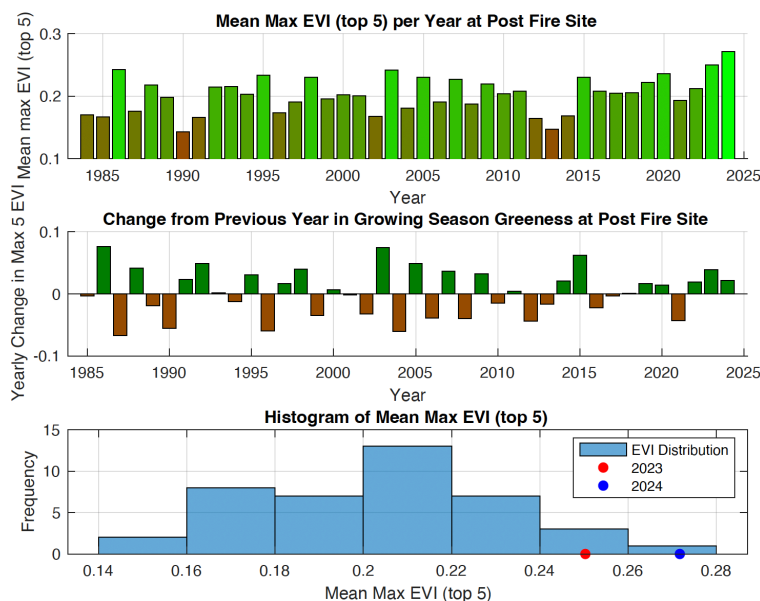


Figure 15a and c: Growing Season Productivity has been the highest on record for the last two years

Figure 15b: Growing Season Productivity has increased every year for the last three years

The Post Fire ignited on June 15, 2024, in Los Angeles and Ventura counties, California, and was fully contained by June 28, 2024. The wildfire scorched 15,563 acres and led to the evacuation of 1,200 residents. It was notable for occurring early in the summer, well before peak fire season. It spread rapidly due to hot and dry wind conditions, but may have also been fueled by high vegetation productivity due to the recent wet winter (Cowen 2024)

To measure growing season productivity at the Post Fire burn area, we again calculated the mean of the annual maximum five EVI values. Our results show that anomalously high vegetation productivity occurred in the three growing seasons leading up

to 2024, which has never before occurred in the area since the beginning of the EVI dataset (Figure 15 a-b). Furthermore, the growing season EVI in 2024 was the highest on record (Figure 15c). This exceptional growing season productivity was likely fueled by two back-to-back anomalously wet winters in 2023 and 2024 (Figure 16).

The Post Fire occurred in a dry, hot, low elevation area, dominated by grasses. This may explain why high vegetation productivity preceded the fire, as grasslands are fuel-limited fire regimes. As the 2024 fire season continues, there are concerns that more grassland fires in California will occur owing to the two wet consecutive winters and dramatic vegetation growth (Cowen 2024), which is especially worrisome if summer EDDI conditions are anomalously high.

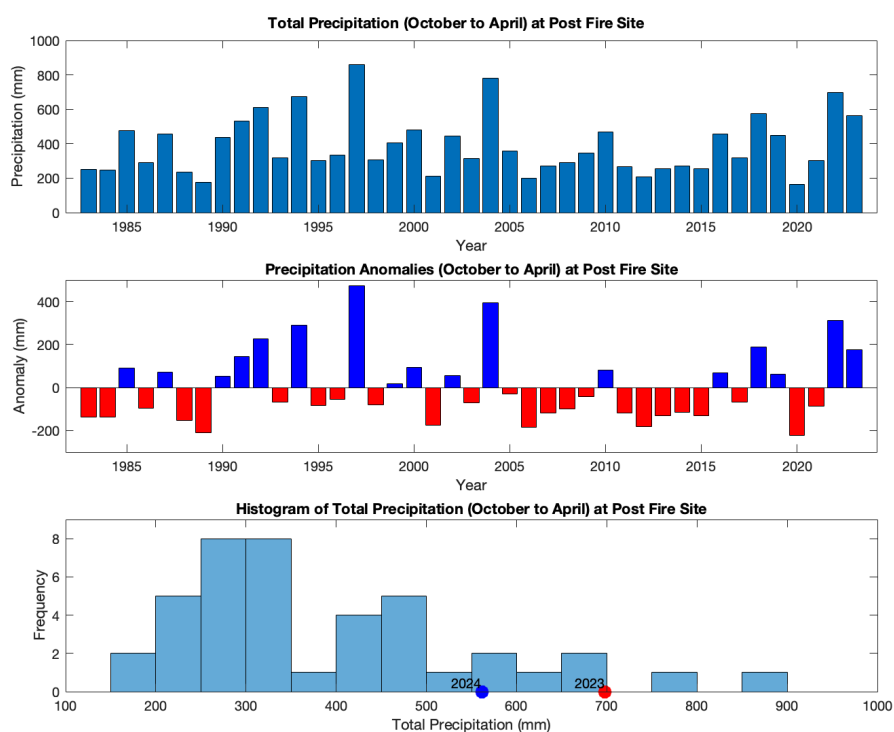


Figure 16: Anomalously high winter precipitation was recorded the last two years at the Post Fire Site

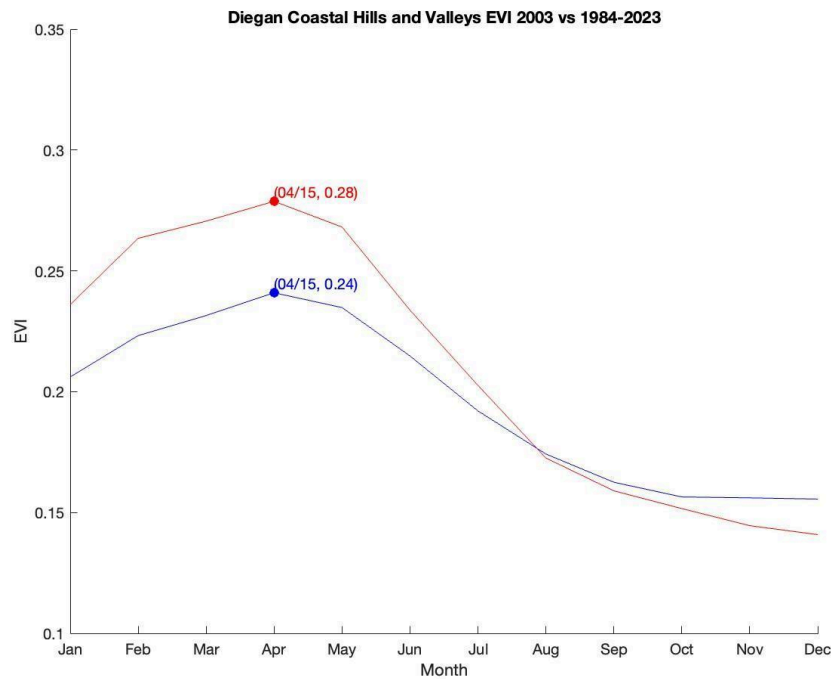


Figure 17: EVI in the Diegan Coastal Hills and Valleys (the site of the 2003 Cedar Fire) in 2003 (red) vs 1984-2023 (blue)

In the Diegan Coastal Hills and Valleys, the ecoregion in which the 2003 Cedar Fire occurred, we found that EVI measurements in 2003 indicated an anomalously productive growing season (Figure 17, shown in red) which was followed by rapid drying in the months leading up to the fire's ignition in October compared to the average EVI cycle (shown in blue). Strong Santa Ana winds combined with this abundance of ready to burn live fuels led to what was at the time the largest wildfire in recorded California history since the Santiago Canyon Fire of 1889 (CAL FIRE 2024).

Summary and Implications

California exhibits a wide range of ecosystems, each with its unique characteristics, vegetation types, growing seasons, and fire behavior. Understanding fire dynamics across these ecosystems allows for tailored fire management strategies that account for ecosystem-specific factors.

Our findings suggest that wet winters may lead to increased wildfire risk in fuel-limited ecosystems like grasslands. This is because anomalously high rainfall can lead to higher biomass accumulation in the growing season. Many shallow-rooted grasses and forbs are unable to access water several months after the end of the rainy season as soils nearer to the surface dry. Additionally, many inland grasslands in California grow on soils that are relatively heavy in clay, which is not porous and can lead to heavy runoff, leading to lower water availability. Furthermore, soils with low organic matter content generally have lower water retention, which further limits the water availability for grasses in the fall.

By contrast, our results indicate that in chaparral-dominated areas, increased winter precipitation leads to conditions that may decrease wildfire risk. Like grasses, we found growing season productivity in chaparral dominant ecosystems to be correlated with winter precipitation. Unlike in grasslands, however, after wet winters chaparral was able to retain most of that relative greenness into the fire season (August-October).. This may indicate that after wet winters, the chaparral is healthier and each plant has more available water in the fire season, which may ultimately reduce wildfire risk despite the greater abundance of biomass. By contrast, after dry winters, the chaparral experienced significant browning, indicating the potential abundance of dry fuel for wildfires.

These results underscore the need for further research to clarify the importance of fuel abundance versus fuel dryness, especially in conifer forest and sage scrub ecoregions for accurate Southern California wildfire risk assessment.

These results have implications for wildfire management and long-lead decision support, which is increasingly important as climate change is expected to enhance drying of vegetation between rain events. This knowledge can guide land-use planning, wildfire prevention efforts, and ecosystem restoration initiatives aimed at fostering resilience in the face of escalating wildfire threats in the region.

While the primary focus of this study is on vegetation communities throughout Southern California, its results could pave the way for broader applications in other wildfire-prone regions that receive substantial winter precipitation from atmospheric rivers. These areas may encompass Northern California, the Pacific Northwest, as well as international regions like Chile, Portugal and Australia, where similar climatic conditions and wildfire challenges are prevalent.

Challenges and Notes for Future Research

This study did not explore the correlations between wildfire area burned (WFAB) and preceding factors such as WP and EDDI due to time constraints. Future studies could incorporate observed WFAB data to better understand this influence.

The US EPA level IV ecoregion shapefile splits ecoregions apart when they are not contiguous. Therefore data had to be combined from multiple regions to create an

ecoregion. In some instances, such as the Northern Channel Islands, this led to the majority, but not the entirety, of the ecoregion being considered. Instead, data was collected considering the two major islands in the chain- Santa Cruz and Santa Rosa Islands.

The tool used to download the data- Climate Engine, uses the Google Earth Engine. Some of the larger ecoregions, for instance 8a, exceeded the computational limits for the engine when considering variables like EVI. Therefore, the time series had to be broken into smaller pieces when downloading the data- for instance, 1984-1998, 2000-2012, and 2012-2023. The Climate Engine API may provide a smoother experience for future studies.

The Level IV Ecoregions themselves contain an abundance of variability. In other words, some are not specific enough to provide an accurate portrayal of the response of specific plant communities to ARs and EDDI. This is both because of variable land cover and plant compositions, variable precipitation across ecoregions, and variable atmospheric conditions. This is especially true in the more mountainous ecoregions, such as the Western Transverse Lower Montane Shrub and Woodland, where the plant communities living at the northern border of the ecoregion are adapted to more desert like conditions, the plant communities at the southern border are adapted to more mediterranean conditions, and the high elevation center of the ecoregion is more akin to a sub-alpine climate. Though it does not yet exist, a level V ecosystem classification system which better separates the variability that exists within level IV ecoregions would be more useful to understand the response of plant communities to precipitation and drought conditions.

While October-April precipitation does consist of majority AR precipitation, some precipitation in this time period comes from other events, such as traditional cold winter

storms out of the north Pacific. Additionally, it is possible to get some AR precipitation outside of this time window.

Furthermore, this study did not examine the cumulative impacts of precipitation. In other words, we did not look at whether two winters of anomalous precipitation led to anomalous EVI measurements. Nor did this study examine atmospheric conditions greater than 180 days into the past. Future studies could factor in longer term EDDI values such as 2 year EDDI.

EVI measures both plant density and greenness but does not distinguish between the two. While anomalously high plant density can indicate high wildfire risk in fuel-limited ecosystems, vegetation greenness can indicate the opposite in climate limited ecosystems. If a metric was created that could distinguish density from greenness, these values would help scientists and land managers better understand fuel loading. If, for instance, plant density was high and plant greenness was low, regardless of whether an ecosystem was fuel or climate limited, this would probably indicate high wildfire risk.

Bibliography

Abatzoglou, John T. “Development of Gridded Surface Meteorological Data for Ecological Applications and Modelling.” *International Journal of Climatology*, vol. 33, no. 1, 21 Dec. 2011, pp. 121–131, <https://doi.org/10.1002/joc.3413>.

Aguilera, R., Luo, N., Basu, R., Wu, J., Clemesha, R., Gershunov, A., & Benmarhnia, T. (2023). A novel ensemble-based statistical approach to estimate daily wildfire-specific PM_{2.5} in California (2006–2020). *Environment International*, 171, 107719.

Albano, Christine M., et al. “Influence of Atmospheric Rivers on Vegetation Productivity and Fire Patterns in the Southwestern U.S.” *Journal of Geophysical Research: Biogeosciences*, vol. 122, no. 2, Feb. 2017, pp. 308–323, <https://doi.org/10.1002/2016jg003608>.

Barbeta, A., Mejía-Chang, M., Ogaya, R., Voltas, J., Dawson, T.E. and Peñuelas, J. (2014). The combined effects of a long-term experimental drought and an extreme drought on the use of plant-water sources in a Mediterranean forest. *Global Change Biology*, 21(3), pp.1213–1225. doi:<https://doi.org/10.1111/gcb.12785>.

Bouchet , R.J. “Evapotranspiration Reelle et Potentielle, Signification Climatique.” *Https://Www.scirp.org/*, IAHS, 1963, www.scirp.org/reference/referencespapers?referenceid=2144306.

Buechi, Hanna. “Long-Term Trends in Wildfire Damages in California.” *The Nature Conservancy* , 2020, emlab.ucsb.edu/sites/default/files/documents/wildfire-brief.pdf.

Cayan, Daniel R., et al. “Autumn Precipitation: The Competition with Santa Ana Winds in Determining Fire Outcomes in Southern California.” *International Journal of Wildland Fire*, vol. 31, no. 11, 25 Oct. 2022, pp. 1056–1067, <https://doi.org/10.1071/wf22065>.

Chen, Zefeng, et al. “Vegetation Response to Precipitation Anomalies under Different Climatic and Biogeographical Conditions in China.” *Scientific Reports*, vol. 10, no. 1, 21 Jan. 2020, <https://doi.org/10.1038/s41598-020-57910-1>.

Chiariello, N.R. and Field, C.B. (2004). Seasonal Effects on Vegetation Greenness of California Grassland During Five Years of Global Change Treatments. AGU Fall Meeting Abstracts, [online] 2004, pp.GC51D1082. Available at: <https://ui.adsabs.harvard.edu/abs/2004AGUFMGC51D1082C/abstract> [Accessed 9 Aug. 2024].

Clemesha, Rachel E S, et al. “A High-Resolution Record of Coastal Clouds and Fog and Their Role in Plant Distributions over San Clemente Island, California.” *Environmental*

Research Communications, vol. 3, no. 10, 1 Oct. 2021, pp. 105003–105003,
<https://doi.org/10.1088/2515-7620/ac2894>.

Corringham TW, Ralph FM, Gershunov A, Cayan DR, Talbot CA (2019) Atmospheric Rivers drive flood damages in the western United States. *Sci Adv* 5(12):eaaz631.
<https://doi.org/10.1126/sciadv.aax4631>

Cowan, J. (2024, June 16). In Southern California, a Wildfire That May Foreshadow a Hazardous Summer. *The New York Times*, Retrieved from
<https://www.nytimes.com/2024/06/16/us/los-angeles-wildfire-post-fire.html>

Dettinger, Michael D., et al. “Atmospheric Rivers, Floods and the Water Resources of California.” *Water*, vol. 3, no. 2, 24 Mar. 2011, pp. 445–478,
www.mdpi.com/2073-4441/3/2/445, <https://doi.org/10.3390/w3020445>.

Dong, Chunyu, et al. “The Season for Large Fires in Southern California Is Projected to Lengthen in a Changing Climate.” *Communications Earth & Environment*, vol. 3, no. 1, 17 Feb. 2022, <https://doi.org/10.1038/s43247-022-00344-6>.

Dong, Chunyu, et al. “Vegetation Responses to 2012–2016 Drought in Northern and Southern California.” *Geophysical Research Letters*, vol. 46, no. 7, 11 Apr. 2019, pp. 3810–3821, <https://doi.org/10.1029/2019gl082137>.

dos Santos, T.B., Ribas, A.F., de Souza, S.G.H., Budzinski, I.G.F. and Domingues, D.S. (2022). Physiological Responses to Drought, Salinity, and Heat Stress in Plants: A Review. *Stresses*, 2(1), pp.113–135. doi:<https://doi.org/10.3390/stresses2010009>.

Funk, Chris, et al. “The Climate Hazards Infrared Precipitation with Stations—a New Environmental Record for Monitoring Extremes.” *Scientific Data*, vol. 2, no. 1, Dec. 2015, <https://doi.org/10.1038/sdata.2015.66>.

Gershunov, Alexander, et al. “Assessing the Climate-Scale Variability of Atmospheric Rivers Affecting Western North America.” *Geophysical Research Letters*, vol. 44, no. 15, 3 Aug. 2017, pp. 7900–7908, <https://doi.org/10.1002/2017gl074175>.

Gershunov, A., T.M. Shulgina, R.E.S. Clemesha, K. Guirguis, D.W. Pierce, M.D. Dettinger, D.A. Lavers, D.R. Cayan, S.D. Polade, J. Kalansky and F.M. Ralph, 2019: Precipitation regime change in Western North America: The role of Atmospheric Rivers. *Nature Scientific Reports*, 9:9944, DOI: 10.1038/s41598-019-46169-w. <https://rdcu.be/bJPK0>

Goforth, Brett. “Densification, Stand-Replacement Wildfire, and Extirpation of Mixed Conifer Forest in Cuyamaca Rancho State Park, Southern California | Fire Research and Management Exchange System.” www.frames.gov, 2008, www.frames.gov/catalog/9560.

Griffith, Glenn E., et al. "Ecoregions of California." Pubs.usgs.gov, 2016, pubs.usgs.gov/publication/ofr20161021.

Guiterman, Christopher H, et al. "Vegetation Type Conversion in the US Southwest: Frontline Observations and Management Responses." *Fire Ecology*, vol. 18, no. 1, 19 May 2022, <https://doi.org/10.1186/s42408-022-00131-w>.

Hernández Ayala, José J., et al. "Antecedent Rainfall, Excessive Vegetation Growth and Its Relation to Wildfire Burned Areas in California." *Earth and Space Science*, vol. 8, no. 9, Sept. 2021, <https://doi.org/10.1029/2020ea001624>.

Hobbins, M.T., Wood, A., McEvoy, D.J., Huntington, J.L., Morton, C., Anderson, M. and Hain, C. (2016). The Evaporative Demand Drought Index. Part I: Linking Drought Evolution to Variations in Evaporative Demand. *Journal of Hydrometeorology*, 17(6), pp.1745–1761. doi:<https://doi.org/10.1175/jhm-d-15-0121.1>.

Huete, A., Didan, K., Miura, T., Rodriguez, E.P., Gao, X. and Ferreira, L.G. (2002). Overview of the radiometric and biophysical performance of the MODIS vegetation indices. *Remote Sensing of Environment*, 83(1-2), pp.195–213. doi:[https://doi.org/10.1016/s0034-4257\(02\)00096-2](https://doi.org/10.1016/s0034-4257(02)00096-2).

Keeley, Jon E., and Alexandra D. Syphard. "Twenty-First Century California, USA, Wildfires: Fuel-Dominated vs. Wind-Dominated Fires." *Fire Ecology*, vol. 15, no. 1, 18 July 2019, <https://doi.org/10.1186/s42408-019-0041-0>.

“Landsat Enhanced Vegetation Index | U.S. Geological Survey.” *Www.usgs.gov*, 2024, www.usgs.gov/landsat-missions/landsat-enhanced-vegetation-index.

Li, Andy X., et al. “Inducing Factors and Impacts of the October 2017 California Wildfires.” *Earth and Space Science*, vol. 6, no. 8, Aug. 2019, pp. 1480–1488, <https://doi.org/10.1029/2019ea000661>.

Li, Zhengpeng, et al. “Assessment of Fire Fuel Load Dynamics in Shrubland Ecosystems in the Western United States Using MODIS Products.” *Remote Sensing*, vol. 12, no. 12, 12 June 2020, p. 1911, <https://doi.org/10.3390/rs12121911>.

Ralph, F. M., Neiman, P. J., Wick, G. A., Gutman, S. I., Dettinger, M. D., Cayan, D. R., & White, A. B. (2006). Flooding on California's Russian River: Role of atmospheric rivers. *Geophysical Research Letters*, 33, L13801. <https://doi.org/10.1029/2006GL026689>

Ralph, F. Martin, et al. “A Scale to Characterize the Strength and Impacts of Atmospheric Rivers.” *Bulletin of the American Meteorological Society*, vol. 100, no. 2, Feb. 2019, pp. 269–289, <https://doi.org/10.1175/bams-d-18-0023.1>.

Rastogi, Bharat, et al. “Spatial and Temporal Patterns of Cloud Cover and Fog Inundation in Coastal California: Ecological Implications.” *Earth Interactions*, vol. 20, no. 15, 1 May 2016, pp. 1–19, <https://doi.org/10.1175/ei-d-15-0033.1>.

Rundel, P.W. (2018). California Chaparral and Its Global Significance. [online]

ResearchGate. Available at:

https://www.researchgate.net/publication/324337489_California_Chaparral_and_Its_Global_Significance.

Shi, Hongrong, et al. “Modeling Study of the Air Quality Impact of Record-Breaking Southern California Wildfires in December 2017.” *Journal of Geophysical Research: Atmospheres*, vol. 124, no. 12, 27 June 2019, pp. 6554–6570, agupubs.onlinelibrary.wiley.com/doi/abs/10.1029/2019JD030472, <https://doi.org/10.1029/2019jd030472>.

“Statistics | CAL FIRE.” *Www.fire.ca.gov*, 2024, www.fire.ca.gov/our-impact/statistics.

Steel, Zachary L., et al. “The Fire Frequency-Severity Relationship and the Legacy of Fire Suppression in California Forests.” *Ecosphere*, vol. 6, no. 1, Jan. 2015, p. art8, <https://doi.org/10.1890/es14-00224.1>.

Syphard, A.D., Radeloff, V.C., Keeley, J.E., Hawbaker, T.J., Clayton, M.K., Stewart, S.I. and Hammer, R.B. (2007). HUMAN INFLUENCE ON CALIFORNIA FIRE REGIMES. *Ecological Applications*, 17(5), pp.1388–1402. doi:<https://doi.org/10.1890/06-1128.1>.

Vose et al. "NOAA Monthly U.S. Climate Gridded Dataset (NClimGrid)."

www.ncei.noaa.gov/www.ncei.noaa.gov/access/metadata/landing-page/bin/iso?id=gov.noaa.ncdc:C00332.

Waring, R.H. and Running, S.W. (1978). Sapwood water storage: its contribution to transpiration and effect upon water conductance through the stems of old-growth Douglas-fir. 1(2), pp.131–140. doi:<https://doi.org/10.1111/j.1365-3040.1978.tb00754.x>.

Williams, Park et al. "Anthropogenic Intensification of Cool-Season Precipitation Is Not yet Detectable across the Western United States." *Journal of Geophysical Research. Atmospheres*, vol. 129, no. 12, 11 June 2024, <https://doi.org/10.1029/2023jd040537>. Accessed 23 July 2024.

Zhang, Zhenhai, et al. "The Relationship between Extratropical Cyclone Strength and Atmospheric River Intensity and Position." *Geophysical Research Letters*, vol. 46, no. 3, 10 Feb. 2019, pp. 1814–1823, <https://doi.org/10.1029/2018gl079071>.

Zhou, Yufei. "Relationship between Vegetation Index and Forest Surface Fuel Load." *IDEAS*, 19 Sept. 2022, ideas.repec.org/a/ags/asagre/338264.html. Accessed 3 June 2024.

Zhu, Yong, and Reginald E Newell. "A Proposed Algorithm for Moisture Fluxes from Atmospheric Rivers." *Monthly Weather Review*, vol. 126, no. 3, Mar. 1998, pp. 725–735, journals.ametsoc.org/view/journals/mwre/126/3/1520-0493_1998_126_0725_apafmf_2.0.co_2.xml,

[https://doi.org/10.1175/1520-0493\(1998\)126%3C0725:APAFMF%3E2.0.CO;2](https://doi.org/10.1175/1520-0493(1998)126%3C0725:APAFMF%3E2.0.CO;2). Accessed 9 Aug. 2024.

Gershunov A, Guzman Morales J, Hatchett B, Aguilera R, Shulgina T, Guirguis K, Abatzoglou J, Cayan D, Pierce D, Williams P, Small I, Clemesha R, Schwarz L, Benmarhnia T, Tardy A (2021) Hot and cold flavors of southern California's Santa Ana winds: their causes, trends, and links with wildfire. *Clim Dyn*. <https://doi.org/10.1007/s00382-021-05802-z>

Kolden C, Abatzoglou J (2018) Spatial distribution of wildfires ignited under katabatic versus non-katabatic winds in Mediterranean Southern California USA. *Fire* 1(2):19.
<https://doi.org/10.3390/fire1020019>

Moritz M, Moody TJ, Krawchuk M, Hughes M, Hall A (2010) Spatial variation in extreme winds predicts large wildfire locations in chaparral ecosystems. *Geophys Res Lett* 37:L04801.
<https://doi.org/10.1029/2009GL041735.1>

Westerling AL, Cayan DR, Brown TJ, Hall BL, Riddle LG (2004) Climate, Santa Ana winds and autumn wildfires in southern California. *Eos Trans Amer Geophys Union* 85:289–296.
<https://doi.org/10.1029/2004EO310001>

Keeley, J.E., Guzman-Morales, J., Gershunov, A., Syphard, A.D., Cayan, D., Pierce, D.W., Flannigan, M. and Brown, T.J. (2021). Ignitions explain more than temperature or

precipitation in driving Santa Ana wind fires. *Science Advances*, 7(30).

doi:<https://doi.org/10.1126/sciadv.abh2262>.

A. Park Williams, McKinnon, K.A., Anchukaitis, K.J., Gershunov, A., Varuolo-Clarke, A.M., Rachel and Liu, H. (2024). Anthropogenic Intensification of Cool-Season Precipitation Is Not Yet Detectable Across the Western United States. *Journal of geophysical research. Atmospheres*, 129(12). doi:<https://doi.org/10.1029/2023jd040537>.

Abatzoglou, J.T. (2011). Development of gridded surface meteorological data for ecological applications and modelling. *International Journal of Climatology*, 33(1), pp.121–131. doi:<https://doi.org/10.1002/joc.3413>.

Albano, C.M., Dettinger, M.D. and Souldard, C.E. (2017). Influence of atmospheric rivers on vegetation productivity and fire patterns in the southwestern U.S. *Journal of Geophysical Research: Biogeosciences*, 122(2), pp.308–323. doi:<https://doi.org/10.1002/2016jg003608>.

Barbeta, A., Mejía-Chang, M., Ogaya, R., Voltas, J., Dawson, T.E. and Peñuelas, J. (2014). The combined effects of a long-term experimental drought and an extreme drought on the use of plant-water sources in a Mediterranean forest. *Global Change Biology*, 21(3), pp.1213–1225. doi:<https://doi.org/10.1111/gcb.12785>.

Bouchet, R.J. (1963). *Evapotranspiration réelle et potentielle, signification climatique*. [online] <https://www.scirp.org/>. Available at: <https://www.scirp.org/reference/referencespapers?referenceid=2144306> [Accessed 21 Jul. 2024].

Buechi, H. (2020). *Long-term trends in wildfire damages in California*. [online] The Nature Conservancy . Available at: <https://emlab.ucsb.edu/sites/default/files/documents/wildfire-brief.pdf> [Accessed 3 Jun. 2024].

Cayan, D.R., DeHaan, L.L., Gershunov, A., Guzman-Morales, J., Keeley, J.E., Mumford, J. and Syphard, A.D. (2022). Autumn precipitation: the competition with Santa Ana winds in determining fire outcomes in southern California. *International Journal of Wildland Fire*, 31(11), pp.1056–1067. doi:<https://doi.org/10.1071/wf22065>.

- Chen, Z., Wang, W. and Fu, J. (2020). Vegetation response to precipitation anomalies under different climatic and biogeographical conditions in China. *Scientific Reports*, 10(1). doi:<https://doi.org/10.1038/s41598-020-57910-1>.
- Chiariello, N.R. and Field, C.B. (2004). Seasonal Effects on Vegetation Greenness of California Grassland During Five Years of Global Change Treatments. *AGU Fall Meeting Abstracts*, [online] 2004, pp.GC51D1082. Available at: <https://ui.adsabs.harvard.edu/abs/2004AGUFMGC51D1082C/abstract> [Accessed 9 Aug. 2024].
- Clemesha, R.E.S., Gershunov, A., Lawson, D.M., Longcore, T., MacDonald, B., Booker, M., Munson, B. and O'Connor, K. (2021). A high-resolution record of coastal clouds and fog and their role in plant distributions over San Clemente Island, California. *Environmental research communications*, 3(10), pp.105003–105003. doi:<https://doi.org/10.1088/2515-7620/ac2894>.
- Dettinger, M.D., Ralph, F.M., Das, T., Neiman, P.J. and Cayan, D.R. (2011). Atmospheric Rivers, Floods and the Water Resources of California. *Water*, [online] 3(2), pp.445–478. doi:<https://doi.org/10.3390/w3020445>.
- Dong, C., MacDonald, G.M., Willis, K., Gillespie, T.W., Okin, G.S. and Williams, A.P. (2019). Vegetation Responses to 2012–2016 Drought in Northern and Southern California. *Geophysical Research Letters*, 46(7), pp.3810–3821. doi:<https://doi.org/10.1029/2019gl082137>.
- Dong, C., Williams, A.P., Abatzoglou, J.T., Lin, K., Okin, G.S., Gillespie, T.W., Long, D., Lin, Y.-H., Hall, A. and MacDonald, G.M. (2022). The season for large fires in Southern California is projected to lengthen in a changing climate. *Communications Earth & Environment*, 3(1). doi:<https://doi.org/10.1038/s43247-022-00344-6>.
- dos Santos, T.B., Ribas, A.F., de Souza, S.G.H., Budzinski, I.G.F. and Domingues, D.S. (2022). Physiological Responses to Drought, Salinity, and Heat Stress in Plants: A Review. *Stresses*, 2(1), pp.113–135. doi:<https://doi.org/10.3390/stresses2010009>.
- Funk, C., Peterson, P., Landsfeld, M., Pedreros, D., Verdin, J., Shukla, S., Husak, G., Rowland, J., Harrison, L., Hoell, A. and Michaelsen, J. (2015). The climate hazards infrared precipitation

with stations—a new environmental record for monitoring extremes. *Scientific Data*, 2(1). doi:<https://doi.org/10.1038/sdata.2015.66>.

Gershunov, A., Shulgina, T., Ralph, F.M., Lavers, D.A. and Rutz, J.J. (2017). Assessing the climate-scale variability of atmospheric rivers affecting western North America. *Geophysical Research Letters*, 44(15), pp.7900–7908. doi:<https://doi.org/10.1002/2017gl074175>.

Goforth, B. (2008). *Densification, stand-replacement wildfire, and extirpation of mixed conifer forest in Cuyamaca Rancho State Park, southern California* | *Fire Research and Management Exchange System*. [online] www.frames.gov. Available at: <https://www.frames.gov/catalog/9560> [Accessed 23 Jul. 2024].

Griffith, G.E., Omernik, J.M., Smith, D.W., Cook, T.D., Tallyn, E., Moseley, K. and Johnson, C.B. (2016). *Ecoregions of California*. [online] pubs.usgs.gov. Available at: <https://pubs.usgs.gov/publication/ofr20161021>.

Guiterman, C.H., Gregg, R.M., Marshall, L., Beckmann, J.J., Phillip, Falk, D.A., Keeley, J.E., Caprio, A.C., Coop, J.D., Fornwalt, P.J., Haffey, C., R. Keala Hagmann, Jackson, S.T., Lynch, A.M., Margolis, E.Q., Marks, C., Meyer, M.D., Safford, H.D., Syphard, A.D. and Taylor, A.H. (2022). Vegetation type conversion in the US Southwest: frontline observations and management responses. *Fire Ecology*, 18(1). doi:<https://doi.org/10.1186/s42408-022-00131-w>.

Hernández Ayala, J.J., Mann, J. and Grosvenor, E. (2021). Antecedent Rainfall, Excessive Vegetation Growth and Its Relation to Wildfire Burned Areas in California. *Earth and Space Science*, 8(9). doi:<https://doi.org/10.1029/2020ea001624>.

Hobbins, M.T., Wood, A., McEvoy, D.J., Huntington, J.L., Morton, C., Anderson, M. and Hain, C. (2016). The Evaporative Demand Drought Index. Part I: Linking Drought Evolution to Variations in Evaporative Demand. *Journal of Hydrometeorology*, 17(6), pp.1745–1761. doi:<https://doi.org/10.1175/jhm-d-15-0121.1>.

Huete, A., Didan, K., Miura, T., Rodriguez, E.P., Gao, X. and Ferreira, L.G. (2002). Overview of the radiometric and biophysical performance of the MODIS vegetation indices. *Remote Sensing of Environment*, 83(1-2), pp.195–213. doi:[https://doi.org/10.1016/s0034-4257\(02\)00096-2](https://doi.org/10.1016/s0034-4257(02)00096-2).

Huete, A.R., Didan, K., Shimabukuro, Y.E., Ratana, P., Saleska, S.R., Hutyra, L.R., Yang, W., Nemani, R.R. and Myneni, R. (2006). Amazon rainforests green-up with sunlight in dry season. *Geophysical Research Letters*, 33(6). doi:<https://doi.org/10.1029/2005gl025583>.

Information (NCEI), N.C. for E. (2014). *NOAA Monthly U.S. Climate Gridded Dataset (NClimGrid)*. [online] www.ncei.noaa.gov. Available at: <https://www.ncei.noaa.gov/access/metadata/landing-page/bin/iso?id=gov.noaa.ncdc:C00332> [Accessed 21 Jul. 2024].

Information (NCEI), N.C. for E. (n.d.). *NOAA Monthly U.S. Climate Gridded Dataset (NClimGrid)*. [online] www.ncei.noaa.gov. Available at: <https://www.ncei.noaa.gov/access/metadata/landing-page/bin/iso?id=gov.noaa.ncdc:C00332>.

Keeley, J.E., Guzman-Morales, J., Gershunov, A., Syphard, A.D., Cayan, D., Pierce, D.W., Flannigan, M. and Brown, T.J. (2021). Ignitions explain more than temperature or precipitation in driving Santa Ana wind fires. *Science Advances*, 7(30). doi:<https://doi.org/10.1126/sciadv.abh2262>.

Keeley, J.E. and Syphard, A.D. (2019). Twenty-first century California, USA, wildfires: fuel-dominated vs. wind-dominated fires. *Fire Ecology*, 15(1). doi:<https://doi.org/10.1186/s42408-019-0041-0>.

Li, A.X., Wang, Y. and Yung, Y.L. (2019). Inducing Factors and Impacts of the October 2017 California Wildfires. *Earth and Space Science*, 6(8), pp.1480–1488. doi:<https://doi.org/10.1029/2019ea000661>.

Li, Z., Shi, H., Vogelmann, J.E., Hawbaker, T.J. and Peterson, B. (2020). Assessment of Fire Fuel Load Dynamics in Shrubland Ecosystems in the Western United States Using MODIS Products. *Remote Sensing*, 12(12), p.1911. doi:<https://doi.org/10.3390/rs12121911>.

Provost, L., Domergue, F., Lalanne, C.C., Patricio Ramos Campos, Grosbois, A., Bert, D., Céline Meredieu, Danjon, F.F., Christophe Plomion and Jean-Marc J.-M. Gion (2013). Soil water stress affects both cuticular wax content and cuticle-related gene expression in young saplings of

maritime pine (*Pinus pinaster* Ait). *BMC Plant Biology*, [online] 13(1), pp.95–95.
doi:<https://doi.org/10.1186/1471-2229-13-95>.

Ralph, F.M., Rutz, J.J., Cordeira, J.M., Dettinger, M., Anderson, M., Reynolds, D., Schick, L.J. and Smallcomb, C. (2019). A Scale to Characterize the Strength and Impacts of Atmospheric Rivers. *Bulletin of the American Meteorological Society*, 100(2), pp.269–289.
doi:<https://doi.org/10.1175/bams-d-18-0023.1>.

Ramírez, J.A. (2005). Observational evidence of the complementary relationship in regional evaporation lends strong support for Bouchet’s hypothesis. *Geophysical Research Letters*, 32(15). doi:<https://doi.org/10.1029/2005gl023549>.

Rastogi, B., A. Park Williams, Fischer, D.T., Iacobellis, S.F., McEachern, K., Carvalho, L.V., Jones, C., Baguskas, S.A. and Still, C.J. (2016). Spatial and Temporal Patterns of Cloud Cover and Fog Inundation in Coastal California: Ecological Implications. *Earth Interactions*, 20(15), pp.1–19. doi:<https://doi.org/10.1175/ei-d-15-0033.1>.

Rundel, P.W. (2018). *California Chaparral and Its Global Significance*. [online] ResearchGate. Available at:
https://www.researchgate.net/publication/324337489_California_Chaparral_and_Its_Global_Significance.

Shi, H., Jiang, Z., Zhao, B., Li, Z., Chen, Y., Gu, Y., Jiang, J.H., Lee, M., Liou, K., Neu, J.L., Payne, V.H., Su, H., Wang, Y., Witek, M. and Worden, J. (2019). Modeling Study of the Air Quality Impact of Record-Breaking Southern California Wildfires in December 2017. *Journal of Geophysical Research: Atmospheres*, [online] 124(12), pp.6554–6570.
doi:<https://doi.org/10.1029/2019jd030472>.

Steel, Z.L., Safford, H.D. and Viers, J.H. (2015). The fire frequency-severity relationship and the legacy of fire suppression in California forests. *Ecosphere*, 6(1), p.art8.
doi:<https://doi.org/10.1890/es14-00224.1>.

Syphard, A.D., Radeloff, V.C., Keeley, J.E., Hawbaker, T.J., Clayton, M.K., Stewart, S.I. and Hammer, R.B. (2007). HUMAN INFLUENCE ON CALIFORNIA FIRE REGIMES. *Ecological Applications*, 17(5), pp.1388–1402. doi:<https://doi.org/10.1890/06-1128.1>.

Waring, R.H. and Running, S.W. (1978). Sapwood water storage: its contribution to transpiration and effect upon water conductance through the stems of old-growth Douglas-fir. 1(2), pp.131–140. doi:<https://doi.org/10.1111/j.1365-3040.1978.tb00754.x>.

www.fire.ca.gov. (2024). *Statistics | CAL FIRE*. [online] Available at: <https://www.fire.ca.gov/our-impact/statistics>.

www.usgs.gov. (2024). *Landsat Enhanced Vegetation Index | U.S. Geological Survey*. [online] Available at: <https://www.usgs.gov/landsat-missions/landsat-enhanced-vegetation-index>.

Zhang, Z., Ralph, F.M. and Zheng, M. (2019). The Relationship Between Extratropical Cyclone Strength and Atmospheric River Intensity and Position. *Geophysical Research Letters*, 46(3), pp.1814–1823. doi:<https://doi.org/10.1029/2018gl079071>.

Zhou, Y. (2022). *Relationship Between Vegetation Index and Forest Surface Fuel Load*. [online] IDEAS. Available at: <https://ideas.repec.org/a/ags/asagre/338264.html> [Accessed 3 Jun. 2024].

Zhu, Y. and Newell, R.E. (1998). A Proposed Algorithm for Moisture Fluxes from Atmospheric Rivers. *Monthly Weather Review*, [online] 126(3), pp.725–735. doi:[https://doi.org/10.1175/1520-0493\(1998\)126%3C0725:APAFMF%3E2.0.CO;2](https://doi.org/10.1175/1520-0493(1998)126%3C0725:APAFMF%3E2.0.CO;2).